ACS Catalysis

Letter

pubs.acs.org/acscatalysis

Controllable Synthesis of Cobalt Monoxide Nanoparticles and the Size-Dependent Activity for Oxygen Reduction Reaction

Jing Liu,[†,∥] Luhua Jiang,*[,†] Bingsen Zhang,[‡] Jutao Jin,[†] Dang Sheng Su,[‡,§] Suli Wang,[†] and Gongquan Sun*[,†]

[†]Dalian National Laboratory for Clean Energy, Dalian Institute of Chemical Physics, Chinese Academy of Sciences, 116023 Dalian, China

[‡]Institute of Metal Research, Chinese Academy of Sciences, 110016 Shenyang, China

[§]Fritz Haber Institute of the Max Planck Society, 14195 Berlin, Germany

[∥]University of the Chinese Academy of Sciences, 100049 Beijing, China

Supporting Information

ABSTRACT: In this work, carbon-supported cobalt monoxides with an average size of 3.5, 4.9, and 6.5 nm are synthesized via a facile colloidal method avoiding any surfactants of long chains. Along with controlling the CoO particle size, we investigate the dependence of ORR activity on particle size of the CoO/C composite. It is discovered that the turnover frequency of the ORR per CoO site is largely independent of the particle size in the range of 3−7 nm, and the enhanced ORR activity for the smaller CoO particles is attributed to the enlarged interface between CoO and carbon.

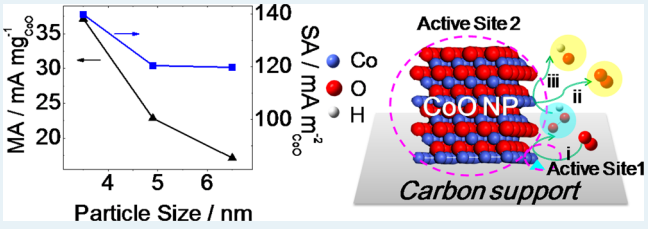

KEYWORDS: *CoO nanoparticles, size-dependent, oxygen reduction reaction, electrocatalyst, alkaline media*

Oxygen reduction reaction (ORR), as the cathodic reaction of fuel cells and metal−air batteries, is of great significance. Although Pt is the most studied and active catalyst presently, exploring cheap alternatives already becomes an urgent task because of the limited resource and the expensive cost of Pt.[1,2] Recently, cobalt oxides supported on graphene are reported as active for the ORR.[3,4] However, the origin of ORR activity of such carbon-supported cobalt oxides is not well understood yet.

For heterogeneous catalysis, particle size of active components usually has significant interplay with the activity.[5] As is well-known, particle size is directly related with surface area and the percentages of different crystal facets in catalysts, both of which have potential impact on the catalytic activity.[6−8]Although size-dependent catalytic activity of nanoparticles (NPs) were extensively reported and understood in heterogeneous catalysis,[9,10] the particle-size effect of cobalt oxide on the ORR activity is rarely studied, most probably due to the challenge to synthesize monodispersed CoO NPs with well-controlled sizes. Traditionally, monodispersed CoO NPs were obtained mainly by thermal decomposition of organic cobalt salts in the presence of capping agents in organic solvents with long hydrocarbon chains.[11,12] The synthesis processes are rather complex and involve expensive and toxic organic cobalt salts as precursors, which limits both its large-scale synthesis and its application. Furthermore, the capping agents are difficult to remove and are prone to masking the active sites and decreasing the electro-activity. Another approach to obtain CoO is pyrolysis of Co_3O_4 in an inert atmosphere, although severe agglomeration of CoO particles occurs during the phase transformation because the temperature required is usually as high as 900 °C for bulk materials.[13]

It is known that the temperature required for phase transformation of particles in nanosize significantly decreases compared with that for the bulk material. Ignited by this point, we propose to synthesize CoO NPs via pyrolyzing CoO_x NPs with well-controlled nanosize. Remarkably, the solid-phase transformation temperature for the CoO_x to CoO phase can be sharply decreased to 500 °C, because the abundant lattice defects in nanosized amorphous CoO_x can afford feasible pathway for atomic diffusion. Moreover, the CoO NPs with well-controlled size are achieved by manipulating the size of the CoO_x NPs. For the first time, the impact of the cobalt monoxide particle size on the ORR activity is investigated. It should be mentioned that carbon often serves as a support for metal oxides to improve the conductivity, whereas its catalysis for the ORR is usually ignored. Herein, the synergetic effect between carbon and cobalt oxides is also discussed.

The typical synthesis process is described as follows: CoO_x colloid was synthesized by refluxing the mixture of cobalt acetate in ethanol (0.08M, 25 mL) and ammonia solution (25 wt %, 2.5 mL) at 100 °C, and then cobalt oxide NPs were

Received: March 8, 2014
Revised: July 30, 2014
Published: July 30, 2014

   dx.doi.org/10.1021/cs500741s | ACS Catal. 2014, 4, 2998−3001

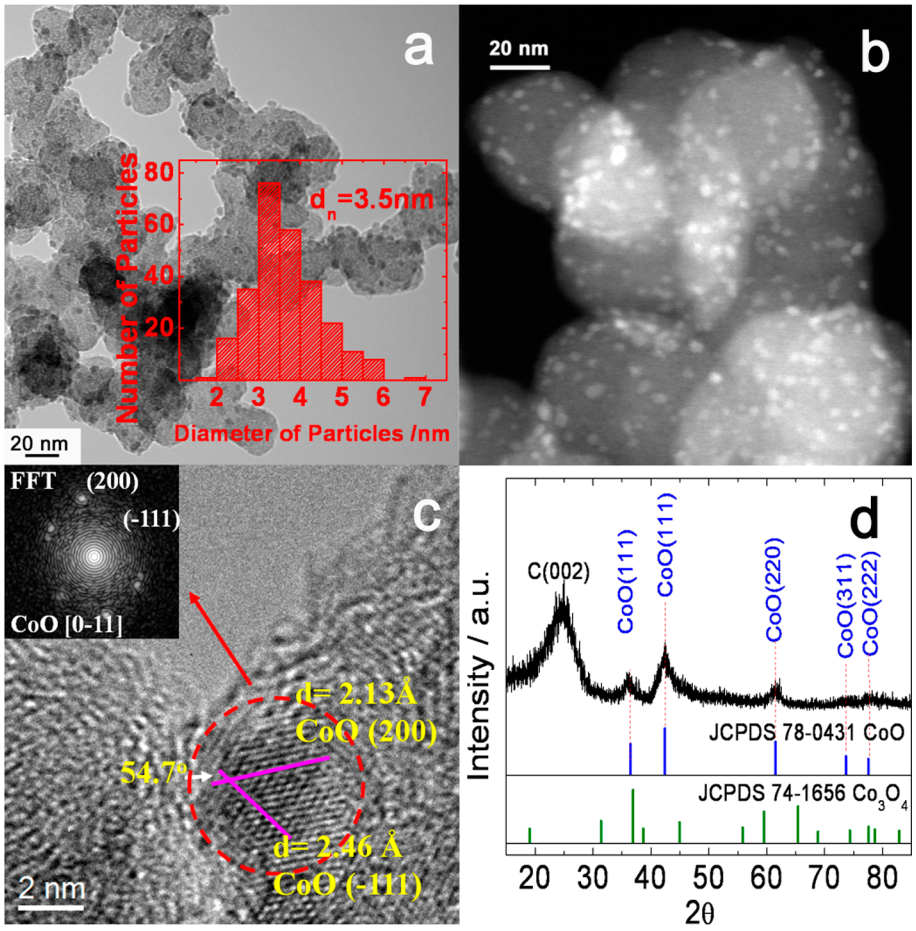

Figure 1. (a) Low magnification bright-field image, (b) HAADF-STEM image, (c) HRTEM image of a single particle, (d) and the XRD pattern of a CoO/C catalyst synthesized with 0.08 M cobalt acetate solution. The insets of (a) and (c) are the corresponding particle distribution histogram and the SAED patterns of the selected particle, respectively.

deposited onto the carbon support to obtain the CoO_x/C composite. The obtained composite was then calcined at 500 °C in N_2 atmosphere for 2 h to get the CoO/C. As displayed in TEM images shown in Figure 1a,b, the resultant ultrafine CoO NPs are uniformly deposited on the carbon support. More than 200 particles are randomly selected for size analysis. The obtained particle size distribution histogram (Figure 1a inset) presents a narrow range with an average size of 3.5 nm. The high-resolution TEM image, shown in Figure 1c, indicates that the CoO NPs display a lattice spacing of 2.46 and 2.16 nm, corresponding to the face-centered cubic (fcc) CoO (111) and (200) planes (JCPDS PDF 78-0431). The selected-area electron diffraction (SAED) pattern (Figure 1c inset) also displays polycrystalline diffraction rings corresponding to the indices of the lattice planes of an fcc-CoO phase. In the XRD pattern of the CoO/C sample as shown in Figure 1d, the typical broadening diffraction peaks from the CoO (111), CoO (200), and CoO (220) indices near 36.5, 42.4, and 61.5° confirms the existence of fcc-CoO nanocrystals, which is consistent with the HRTEM analysis. The peak centered at 25.6° comes from the diffraction of graphite (002) of carbon. The Co species on the surface of the fresh CoO/C sample (stored in glovebox for less than 2 weeks), as indicated by the Co 2p XPS spectrum (Supporting Information (SI), Figure S1), is mainly Co (II).

As stated above, in this synthesis procedure, it is critical to control the particle size of the precursor CoO_x NPs to obtain CoO NPs with controlled particle size. Thus, finely controlling the nucleation and growth processes of the CoO_x are necessary. By employing ethanol as solvent and ammonia as precipitator, we obtain ultrafine monodispersed CoO_x NPs. The beneficial roles of ethanol and ammonia lie in two aspects: first, the hydrolysis rate of cobalt salt can be well controlled by ammonia, which releases hydroxyl ions slowly in ethanol with temperature increasing; second, ammonia molecules tend to be strongly chelated with cobalt ions, working as a capping agent to hinder the particle growth. Furthermore, by simply changing the concentration of cobalt acetate solution, the size of CoO_x NPs can be tuned. With the concentration of cobalt acetate solution varying from 0.04, 0.08 to 0.20 M, the size of the obtained CoO_x NPs are 1.5, 2, and 3.5 nm, respectively (SI, Figure S2). The as-prepared CoO_x colloid is amorphous as demonstrated by the XRD pattern (SI, Figure S3). When being thermally treated in N_2 atmosphere, the amorphous CoO_x NPs might incessantly release oxygen and be reduced as indicated by the TG profile of the CoO_x/C (SI, Figure S4). Amorphous CoO_x NPs can be converted into pure fcc-CoO phase after thermal treatment at 500 °C. Nevertheless, it is observed that the size of the CoO NPs increased to some extent comparing with that of the corresponding CoO_x precursor due to Oswald ripening suffering from the thermal treatment. The average particle size of CoO NPs obtained from the CoO_x precursor of 1.5, 2, and 3.5 nm is 4.9, 3.5, and 6.5 nm, respectively (SI, Figure S5). Surprisingly, the CoO_x with the smallest particle

dx.doi.org/10.1021/cs500741s | ACS Catal. 2014, 4, 2998−3001

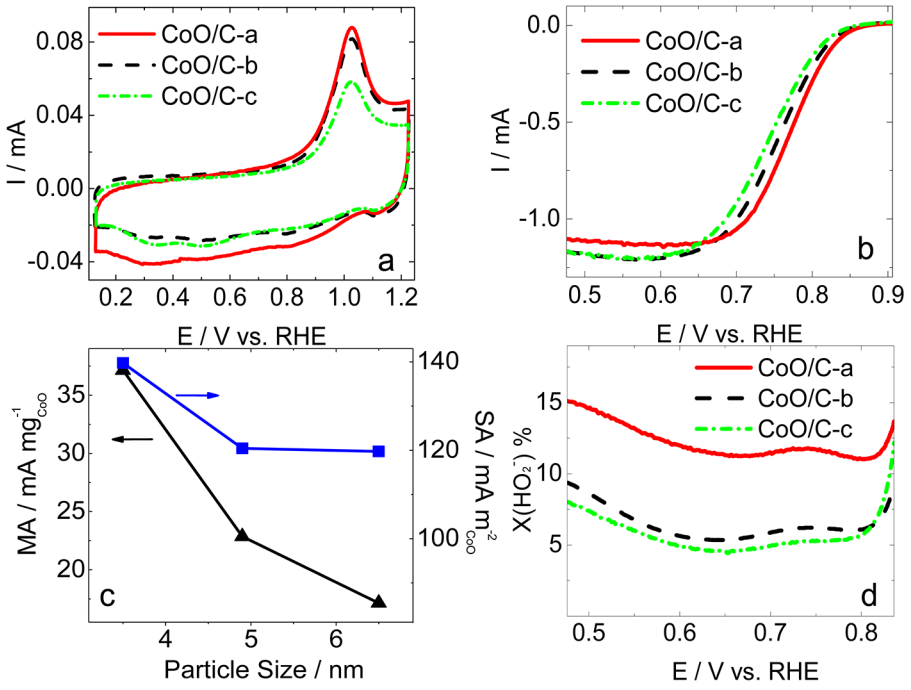

Figure 2. Electrochemical properties of CoO/C catalysts. (a) Cyclic voltammograms in N_2-saturated 0.1 M NaOH. (b) The ORR polarization curves in O_2-saturated 0.1 M NaOH at the rotating rate of 1600 rpm. (c) Dependence of the mass activity and the specific activity of ORR on varied CoO particle size at potential of 0.8 V. (d). The HO_2^- production as the function of potential obtained from RRDE results.

size of 1.5 nm grows a bit more than the other two samples, possibly because the smallest particles are too populated, and therefore, it easily agglomerates during the thermal treatment. Consequently, the CoO_x colloid precursor with the medium size produces CoO with the smallest particle size. For simplicity, the CoO/C composites with the CoO of 3.5, 4.9, and 6.5 nm are denoted as CoO/C-a, CoO/C-b, and CoO/C-c, respectively.

The electrochemical surface features of the CoO/C with different sizes are characterized by cyclic voltammetry in N_2-saturated 0.1 M NaOH (Figure 2a). All samples show a pronounced peak at around 1.0 V, which is attributed to the oxidation of Co (II) to Co (III) on particle surface in the electrolyte solution through $3Co^{2+} + 8OH^- \rightarrow Co_3O_4 + H_2O + 2e^-$.[14] The Co (II)/Co (III) redox couple is proposed concurrent with the ORR.[15] The charge by integrating the oxidizing peak, following the order of CoO/C-a (1.98×10^{-3} C) > CoO/C-b (1.83×10^{-3} C) > CoO/C-c (1.41×10^{-3} C), roughly represents the amount of the electrochemically available redox centers at the surface, suggesting more available redox centers at the surface of the smaller CoO particles.

To examine the dependence of the electrocatalytic ORR activity on the CoO particle size, RDE experiments were performed (Figure 2b). The three CoO/C catalysts exhibit well-defined ORR polarization curves with onset potential starting at 0.87 V. The oxygen reduction currents increase as the potential becomes negative until reaching an O_2 diffusion-controlled plateau. The half-wave potential ($E_{1/2}$) taken at 0.60 mA where the ORR current reaches half of the limiting current for the three catalysts follows a sequence of CoO/C-a (0.77 V) > CoO/C-b (0.76 V) > CoO/C-c (0.74 V), which shows clearly that the oxygen reduction activity varies with the CoO particle size. For a quantitative comparison, the ORR mass activity (MA), normalized to the mass of CoO on electrode, and the specific activity (SA), normalized to the theoretical surface area of the CoO assuming spherical NPs and all surfaces being electrochemical available, are plotted as a function of the particle size in Figure 2c, and the values are listed in SI, Table S1. As can be seen, the MA of the CoO_x/C for the ORR increases with diminishing the particle size, indicating the enhancement of the metal utilization. The SA first decreases as the CoO particle size increases from 3.5 to 4.9 nm and then remains essentially unchanged with the particle size further increasing to 6.5 nm, suggesting that the ORR activity per CoO site varies little as the CoO particle size is less than 10 nm. On the basis of this result, it is deduced that the enhanced ORR activity is correlated to the improvement in metal utilization, not the turnover frequency per CoO site.

Further RRDE measurements were carried out to detect the HO_2^- yield over the three CoO/C samples. As shown in Figure 2d, all samples show a low production of HO_2^-, indicating an apparent $4e^-$ process toward ORR. However, we surprisingly found that the most active sample (i.e., CoO/C-a, the one with the smallest CoO average particle size), produces the highest content of HO_2^- (corresponding to the lowest electron transfer number). This motivates us to discover the ORR pathway over the CoO/C composite. For such an apparent $4e^-$ process, we have recently elucidated an associative pathway over the CoO_x/C catalyst,[16] which involves the following reactions: (i) $O_2 + H_2O + 2e^- \rightarrow HO_2^- + OH^-$; (ii) $2HO_2^- \rightarrow O_2 + 2OH^-$; and (iii) $HO_2^- + H_2O + 2e^- \rightarrow 3OH^-$. That is, at the low overpotential region ($E > 0.7$ V), the apparent $4e^-$ ORR process involves reactions (i) and (ii); however, at the high overpotential region ($E < 0.7$ V), the $4e^-$ ORR process involves all the three reactions. Considering the similarities of the CoO_x/C and the CoO/C, it is speculated that a similar ORR pathway proceeds over the CoO/C catalyst, as described in Scheme 1. This is also supported by the fact that the HO_2^- yield decreases with increasing the thickness of the CoO/C film over the GC electrode (SI, Figure S6). To further identify the

dx.doi.org/10.1021/cs500741s | ACS Catal. 2014, 4, 2998−3001

Scheme 1. ORR Mechanism on the CoO/C Catalyst (Side View)

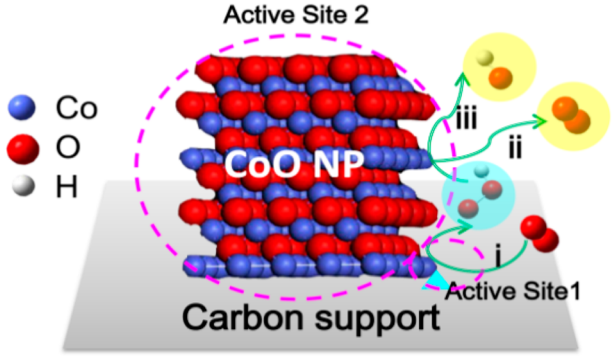

active site for reactions (i–iii), the ORR polarization curves over carbon support and CoO NPs are tested, respectively (SI, Figure S7). Both show much more negative onset potentials and lower ORR currents than the CoO/C composite. Additionally, the CV of the CoO NPs shows no obvious peak of Co(II)/Co(III) and weak oxidation current, possibly due to the rather small electrochemically available surface of the agglomerated CoO NPs. On the basis of the above fact combined with the observation that reducing the CoO NP size leads to enhancement of the ORR mass activity and also the HO_2^- production, it can be concluded that the promoted ORR current over the smallest CoO particles benefits from the enlargement of the interface between carbon support and CoO NPs. Therefore, the interface between carbon and CoO NPs can be identified as the most active site (Active Site 1) for the first $2e^-$ reduction of oxygen to form HO_2^-. Because carbon is known to be inert regardless of whether chemical disproportationation (Reaction (ii)) or electro-reduction reaction of HO_2^- (Reaction (iii)) occurs,[16−18] it is deduced that reaction (ii) and (iii) probably take place on the CoO NPs (Active Site 2). On the basis of the proposed ORR mechanism, the observation of higher HO_2^- production over the smaller CoO NPs is explained as follows: for smaller CoO particles, the larger interface between CoO and carbon support produce a great amount of HO_2^- at low overpotentials. Although most of the HO_2^- could instantaneously decompose to oxygen and enter the recycling, resulting in low "apparent" HO_2^- yields for the three samples, the significantly higher HO_2^- amount over CoO/C-a would finally lead to higher "apparent" HO_2^- yields than CoO/C-b and CoO/C-c.

Finally, it should be mentioned that the Co (II) would transform to Co (III) in the oxidative environment, as detected by XRD (SI, Figure S8) and XPS (SI, Figure S9) if the CoO/C sample emerges in O_2-saturated alkaline solution for over 12 h or is stored in air for more than 1 year; however, the fresh sample contains mainly Co (II). We will discuss the influence of crystalline structures of cobalt oxides on the ORR performance in detail later.

In summary, a new strategy to synthesize ultrafine (sub 10 nm) CoO with a controllable particle size via a combined controllable hydrolysis and thermal treatment process is proposed. The CoO/C with smaller CoO particle size exhibits higher ORR activity due to the abundant interface between CoO NPs and carbon supports promoting the rate of oxygen reduction. We believe that the synthetic strategy reported in this work can be further extended to develop other metal oxides for various applications, such as batteries, supercapacitors, and sensors. The ORR mechanism discovered over the CoO/C composite provides guidance for catalyst design.

■ ASSOCIATED CONTENT

Supporting Information

Experimental, XPS spectra (Figures S1 and S9), TEM images (Figures S2 and S5), XRD patterns (Figures S3 and S8), TG profile (Figures S4), RRDE measurements (Figure S6), ORR polarization curves (Figure S7), and Table S1 are included. This material is available free of charge via the Internet at http://pubs.acs.org.

■ AUTHOR INFORMATION

Corresponding Authors

*E-mail: sunshine@dicp.ac.cn.

*E-mail: gqsun@dicp.ac.cn.

Notes

The authors declare no competing financial interest.

■ ACKNOWLEDGMENTS

This work was financially supported by the National Basic Research Program of China (2012CB215500), the "Strategic Priority Research Program" of the Chinese Academy of Sciences (XDA09030104), and Natural Science Foundation of China (20973169, 201106142).

■ REFERENCES

(1) Bing, Y.; Liu, H.; Zhang, L.; Ghosh, D.; Zhang, J. *Chem. Soc. Rev.* **2010**, *39*, 2184–2202.
(2) Rabis, A.; Rodriguez, P.; Schmidt, T. J. *ACS Catal.* **2012**, *2*, 864–890.
(3) Liang, Y.; Li, Y.; Wang, H.; Zhou, J.; Wang, J.; Regier, T.; Dai, H. *Nat. Mater.* **2011**, *10*, 780–786.
(4) He, Q.; Li, Q.; Khene, S.; Ren, X.; López-Suárez, F. E.; Lozano-Castelló, D.; Bueno-López, A.; Wu, G. *J. Phys. Chem. C* **2013**, *117*, 8697–8707.
(5) Przybylski, K.; Smeltzer, W. W. *J. Electrochem. Soc.* **1981**, *128*, 897–902.
(6) Esswein, A. J.; McMurdo, M. J.; Ross, P. N.; Bell, A. T.; Tilley, T. D. *J. Phys. Chem. C* **2009**, *113*, 15068–15072.
(7) Kinoshita, K. *J. Electrochem. Soc.* **1990**, *137*, 845–848.
(8) Kaur, R.; Pal, B. *J. Mol. Catal. A: Chem.* **2012**, *355*, 39–43.
(9) Hutchings, G. J.; Haruta, M. *Appl. Catal., A* **2005**, *291*, 2–5.
(10) Kuhn, J. N.; Huang, W.; Tsung, C.-K.; Zhang, Y.; Somorjai, G. A. *J. Am. Chem. Soc.* **2008**, *130*, 14026–14027.
(11) Zhang, Y.; Zhu, J.; Song, X.; Zhong, X. *J. Phys. Chem. C* **2008**, *112*, 5322–5327.
(12) Seo, W. S.; Shim, J. H.; Oh, S. J.; Lee, E. K.; Hur, N. H.; Park, J. T. *J. Am. Chem. Soc.* **2005**, *127*, 6188–6189.
(13) Tang, C.-W.; Wang, C.-B.; Chien, S.-H. *Thermochim. Acta* **2008**, *473*, 68–73.
(14) Liang, Y.; Wang, H.; Diao, P.; Chang, W.; Hong, G.; Li, Y.; Gong, M.; Xie, L.; Zhou, J.; Wang, J.; Regier, T. Z.; Wei, F.; Dai, H. *J. Am. Chem. Soc.* **2012**, *134*, 15849–15857.
(15) Qin, H.; Lao, S.; Liu, Z.; Zhu, J.; Li, Z. *Int. J. Hydrogen Energy* **2010**, *35*, 1872–1878.
(16) Liu, J.; Jiang, L.; Tang, Q.; Zhang, B.; Su, D. S.; Wang, S.; Sun, G. *ChemSusChem* **2012**, *5*, 2315–2318.
(17) Geniès, L.; Faure, R.; Durand, R. *Electrochim. Acta* **1998**, *44*, 1317–1327.
(18) Hossain, M. S.; Tryk, D.; Yeager, E. *Electrochim. Acta* **1989**, *34*, 1733–1737.